Journal of Nuclear Materials 408 (2011) 67–72

Contents lists available at ScienceDirect

Journal of Nuclear Materials

journal homepage: www.elsevier.com/locate/jnucmat

Effect of hydride orientation on fracture toughness of Zircaloy-4 cladding

Hsiao-Hung Hsu [a,b,*], Leu-Wen Tsay [b]

[a] Institute of Nuclear Energy Research (INER), Lungtan Township, Taoyuan County 325, Taiwan
[b] Institute of Materials Engineering, National Taiwan Ocean University, Keelung 202, Taiwan

ARTICLE INFO

Article history:
Received 15 September 2010
Accepted 31 October 2010

ABSTRACT

Hydrogen embrittlement is one of the major degradation mechanisms for high burnup fuel cladding during reactor service and spent fuel dry storage, which is related to the hydrogen concentration, morphology and orientation of zirconium hydrides. In this work, the *J*-integral values for X-specimens with different hydride orientations are measured to evaluate the fracture toughness of Zircaloy-4 (Zry-4) cladding. The toughness values for Zry-4 cladding with various percentages of radial hydrides are much smaller than those with circumferential hydrides only in the same hydrogen content level at 25 °C. The fractograghic features reveal that the crack path is influenced by the orientation of zirconium hydride. Moreover, the fracture toughness measurements for X-specimens at 300 °C are not sensitive to a variation in hydride orientation but to hydrogen concentration.

1. Introduction

Zircaloy-4 (Zry-4), one of zirconium alloys, has been used as nuclear fuel cladding of light-water reactors for many years because of its neutron transparency, satisfied mechanical strength and corrosion resistance during operation. For the sake of better fuel economy, the nuclear industry is pushing to extend the fuel burnup to higher levels. With burnup extension, an increase in hydrogen concentration and internal pressure of fuel cladding could exacerbate the hydrogen embrittlement of Zircaloy cladding as a result of the attendant variation of hydride orientation and distribution during reactor service and dry storage.

Hydrogen in zirconium alloys has a low solubility and will precipitate in a form of brittle zirconium hydride when the solubility limit is exceeded. The mechanical properties and fracture toughness degrade with precipitation of brittle zirconium hydrides [1,2]. The hydrogen embrittlement of Zircaloy cladding depends not only on the hydrogen concentration, but also on the morphology and orientation of zirconium hydrides [3]. In the 1960s, the post-irradiation examination (PIE) results for failed fuel rods of the Savannah River plant showed that there existed radial zirconium hydrides in front of cracks, and that the cladding ductility degraded remarkably [4]. During reactor operation, zirconium hydrides could be reoriented from the circumferential direction into the radial one when the fuel cladding was subjected to thermal cycling under a hoop stress of sufficient magnitude [5,6]. The presence of radial hydrides could prompt the fuel failure. In the 1990s, the observations that radial zirconium hydrides were mainly located around the crack tips of axially split fuel cladding in Boiling Water Reactors (BWRs) further confirmed that radial hydrides would aggravate the hydrogen embrittlement of Zircaloy cladding [7]. Some of the fractographic features of the axially split fuel cladding were similar to those observed with failed fuel rods of the Savannah River plant. From the above fuel failure cases, it was concluded that radial hydrides could play a crucial role in the axial split of Zircaloy cladding. As is often the case, with the extension of fuel burnup, there are more radial hydrides precipitated in Zircaloy cladding, which is a concern of fuel integrity at higher burnups. So it is of technical interest to investigate and quantify the effects of radial hydrides on the degradation of Zircaloy fuel cladding fracture properties.

In this work, it was intended to study the effect of radial hydride on fracture behavior of Zircaloy cladding with 300 wppm hydrogen concentration. The fracture toughness for the as-hydrided cladding sample was measured by an X-specimen test method [8] to evaluate the effect of radial hydride on the degradation of Zry-4 cladding fracture toughness.

2. Experimental

2.1. Materials

The experiments were conducted on tubing samples fabricated from the stress-relief annealed (SRA) Zry-4 cladding with an outer diameter of 9.5 mm and wall thickness of 0.57 mm. A summary of the principal alloying elements is given in Table 1.

---

* Corresponding author at: Institute of Nuclear Energy Research (INER), Lungtan Township, Taoyuan County 325, Taiwan. Tel.: +886 3 471 1400x6611; fax: +886 3 471 1409.

E-mail address: hhhsu@iner.gov.tw (H.-H. Hsu).

0022-3115/$ - see front matter © 2010 Elsevier B.V. All rights reserved.
doi:10.1016/j.jnucmat.2010.10.068

Table 1
Chemical compositions of Zry-4 cladding.

Specification	Chemical composition					
Element	Cr	Fe	O	Si	Sn	Zr
wt.%	0.11	0.21	0.12	<0.01	1.2	Balance

2.2. Hydrides reorientation

Firstly, Zry-4 cladding samples with uniformly circumferential hydrides were obtained by hydrogen-charging with a thermal cycling process to the target hydrogen concentration levels such as 300 and 500 wppm, which were measured by an inert-gas fusion method using a LECO RH404 hydrogen analyzer [2].

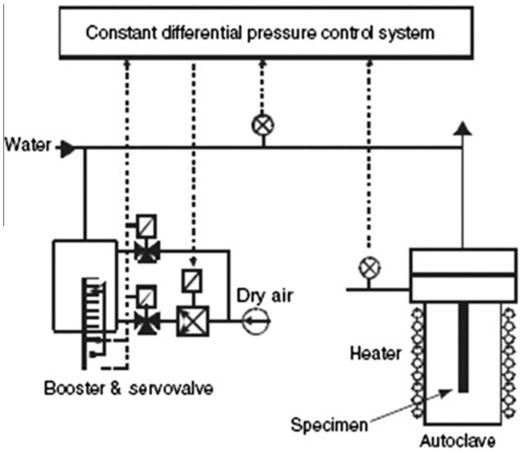

Fig. 1. Schematic diagram of the constant differential pressure control system [9].

The circumferential hydrides in the as-hydrided cladding with a hydrogen content of 300 wppm were further reoriented into radial hydrides by thermal cycling under a constant hoop stress by regulating the differential pressure using a constant differential pressure control system, as schematically shown in Fig. 1 [9]. Then the hydrided cladding specimens were examined by optical metallography to reveal the hydride morphology and orientation. Following the standard metallographic preparation practice, the specimens were etched with an etchant of HF, HNO_3, H_2SO_4 and H_2O in a volume ratio of 1:10:10:10.

2.3. X-specimen test

The X-specimen was designed to measure the fracture toughness of thin-walled tubing with a simulated axial crack, as shown in Fig. 2. Two curved CT specimens machined from a cladding section were glued back to make an X-specimen with high temperature strain gauge cement. The X-specimen test was performed on an MTS model 810 hydraulic mechanical testing machine according to ASTM E 1737–96 standard [10]. For tests at 300 °C, specimens were heated by a chamber furnace at a slow heating rate to the test temperature and then held for about 150 min prior to the start of a test. The furnace temperature was stable to within ± 2 °C.

3. Results and discussion

3.1. Analysis of hydride orientation

The hydride stringers in the uniformly hydrided cladding specimens were precipitated along the circumferential direction as

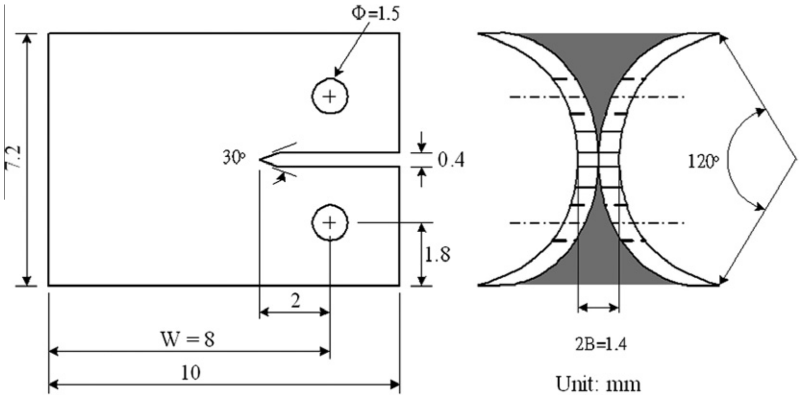

Fig. 2. Configuration and dimensions of an X-specimen for Zry-4 cladding.

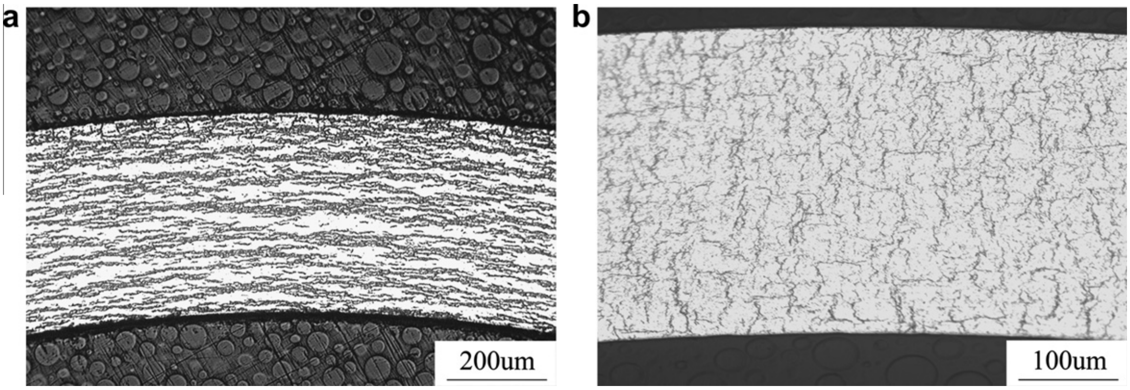

Fig. 3. Optical micrographs showing 300-wppm hydrogen Zry-4 cladding with (a) circumferential hydrides and (b) 52.2% radial hydrides.

shown in Fig. 3a. After the stress reorientation process, some of the hydride platelets were reoriented into the cladding radial direction as shown in Fig. 3b. The percentage of radial hydrides of an X-specimen was an average of those for the neighboring sections, which were separately determined by calculating the fractional area of radial stringers on its photomicrograph [9]. The hydrogen concentration and radial hydride percentage of X-specimens were summarized in Table 2.

3.2. P-LLD curve and J-integral calculation

The Load and load-line displacement (P-LLD) curves obtained for the hydrided cladding by X-specimen test at 25 °C are illustrated in Fig. 4. The values of the maximum load and the load-line displacement level at the maximum load for X-specimens with radial hydrides at 25 °C decreased significantly, compared to those with circumferential hydrides.

The slopes of the P-LLD curves and the values of the maximum loads for X-specimens at 300 °C, as shown in Fig. 5, increased sequentially from those with no hydrides, circumferential hydrides, and radial hydrides of higher percentages to lower percentages. In general, the load-line displacement levels obtained at the maximum loads for the hydrided specimens at 300 °C were larger than those at 25 °C. This could be attributed to the better ductility of zirconium alloys at 300 °C.

Because of the strict limits on the specimen size, especially thickness, required by ASTM standards, a critical J value cannot be applied to the X-specimen test. For comparison purpose, the J-integral evaluated at the maximum load, referred as J_{max}, was used in this work, instead of critical J, to characterize the fracture toughness of Zry-4 cladding specimens whose dimensions cannot meet the ASTM criteria [11]. For an X-specimen of a given thickness and with an initial crack length, the J value was calculated by an equation as follows [12]:

$$J = \beta A_T / Bb \qquad (1)$$

where A_T is total area under the P-LLD curve, B is the specimen thickness, and b is the remaining ligament length. The coefficient β can be expressed by a simplified equation as $\beta = 2(1 + \alpha)/(1 + \alpha^2)$, and the α value depends on the ratio a/b as described by

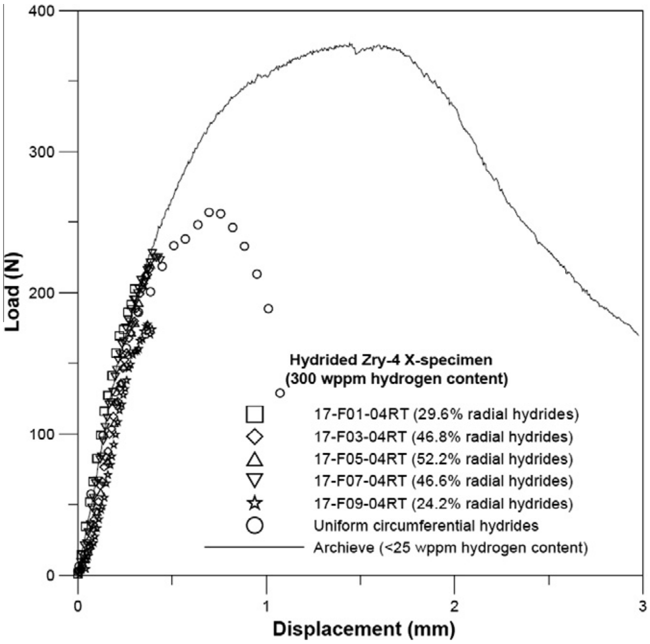

Fig. 4. P-LLD curves for 300-wppm hydrogen Zry-4 cladding with various percentages of radial hydrides by X-specimen test at 25 °C.

the equation, $\alpha = 2[(a/b)^2 + (a/b) + (1/2)]^{1/2} - 2[(a/b) + (1/2)]$, where a is the crack extension.

The schematic P-LLD curve illustrated the areas used in J_{max} estimation was shown in Fig. 6. The total area A_T under the curve can be expressed by $A_T = A_{el} + A_{pl}$, where A_{el} and A_{pl} are the areas under the elastic and plastic parts of the P-LLD curve, respectively. The applied J_{max} value can be divided into elastic and plastic components as $J_{max} = J_{max(el)} + J_{max(pl)}$ related with $A_T = A_{el} + A_{pl}$. Using Eq. (1), the J_{max} values obtained for Zry-4 cladding specimens by X-specimen test are summarized in Table 2.

3.3. Effect of radial hydride

The J_{max} values for hydrided Zry-4 cladding at the 300-wppm hydrogen level against the radial hydride percentages are plotted

Table 2
J_{max} values for hydrided Zry-4 cladding by X-specimen test.

No.	Temperature (°C)	a/W	Hydrogen contents (wppm)	Radial hydrides/total hydrides (%)	J_{max} ($J_{max(el)} + J_{max(pl)}$) (kJ/m^2)
As-received[a]	25		<25	0	115 (32 + 83)
As-received[a]	300		<25	0	97 (24 + 73)
173-R02	25	0.504	300	0	40 (18 + 22)
173-R03	25	0.533	300	0	36 (10 + 26)
175-R01	25	0.500	500	0	21 (11 + 10)
175-R02	25	0.492	500	0	38 (19 + 19)
173-H02	300	0.555	300	0	83 (27 + 56)
173-H03	300	0.548	300	0	80 (26 + 54)
175-H02	300	0.555	500	0	72 (27 + 45)
175-H03	300	0.546	500	0	74 (28 + 46)
17-F01–04RT	25	0.498	300	29.6	9 (7 + 2)
17-F01–06HT300	300	0.505	300	29.6	80 (28 + 52)
17-F03–04RT	25	0.500	300	46.8	11 (10 + 1)
17-F03–05HT300	300	0.495	300	46.8	82 (21 + 61)
17-F05–04RT	25	0.480	300	52.2	11 (11 + 0)
17-F05–05HT300	300	0.519	300	52.2	57 (19 + 38)
17-F07–04RT	25	0.488	300	46.6	14 (9 + 5)
17-F07–05HT300	300	0.497	300	46.6	80 (25 + 55)
17-F09–04RT	25	0.483	300	24.2	9 (8 + 1)
17-F09–05HT300	300	0.473	300	24.2	82 (27 + 55)

[a] An average of J_{max} values was measured by X-specimen test [2].

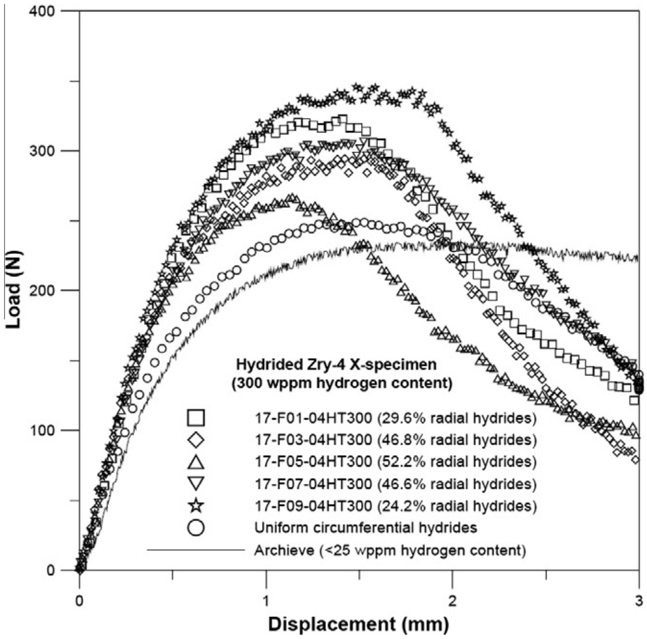

Fig. 5. P-LLD curves for 300-wppm hydrogen Zry-4 cladding with various percentages of radial hydrides by X-specimen test at 300 °C.

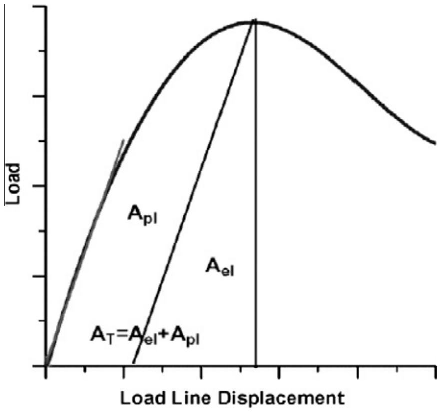

Fig. 6. Schematic P-LLD curve illustrating the areas used in J_{max} calculations.

in Fig. 7. The J_{max} values obtained at 25 °C with radial hydrides at 300-wppm hydrogen level were in the range of 9 and 14 kJ/m^2 and much lower than those with only circumferential hydrides in the hydrogen concentration levels of 300 and 500 wppm. The fracture toughness for Zry-4 cladding became degraded when radial hydrides were present, irrespective of radial hydride percentages. Moreover, the $J_{max(pl)}$ values for Zry-4 cladding with radial hydrides were very small in comparison to those with circumferential hydrides at 25 °C, as demonstrated by Fig. 8. The dramatic decrease of the $J_{max(pl)}$ values for X-specimens with radial hydrides at 25 °C suggested that the radial hydrides played a crucial role in the embrittlement process of Zry-4 cladding.

As shown in Fig. 7, the J_{max} values for X-specimens with the radial hydrides of various percentages at 300 °C were in the same level as those with only circumferential hydrides, except the one with 52.2% radial hydrides. The J_{max} value for the hydrided specimen at 300 °C was larger than that at 25 °C, which could be accounted for by the better ductility of Zry-4 cladding and a part of hydrides redissolved into the metal matrix at 300 °C [13,14]. The cladding containing zirconium hydrides suffered a loss of fracture

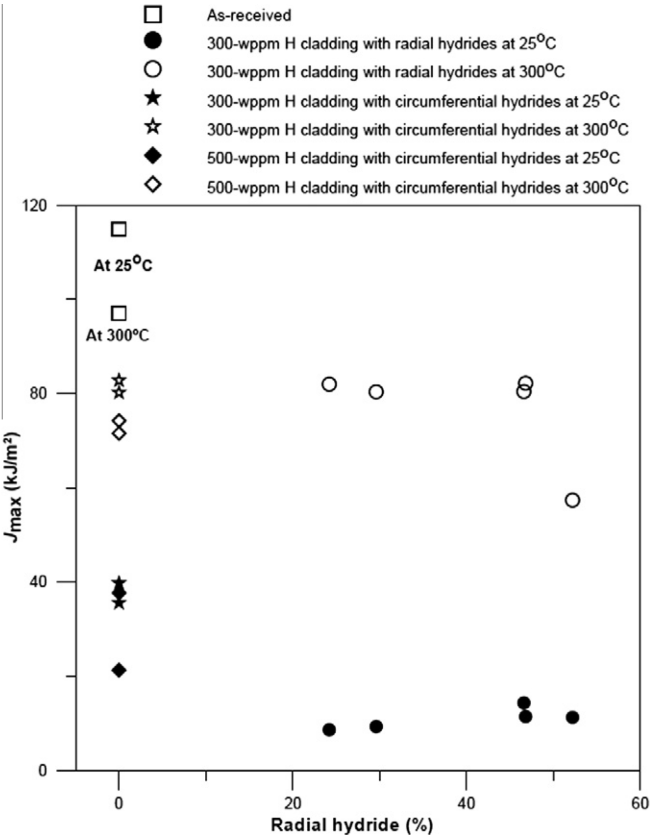

Fig. 7. J_{max} against the radial hydride percentage for Zry-4 cladding at 25 °C and 300 °C.

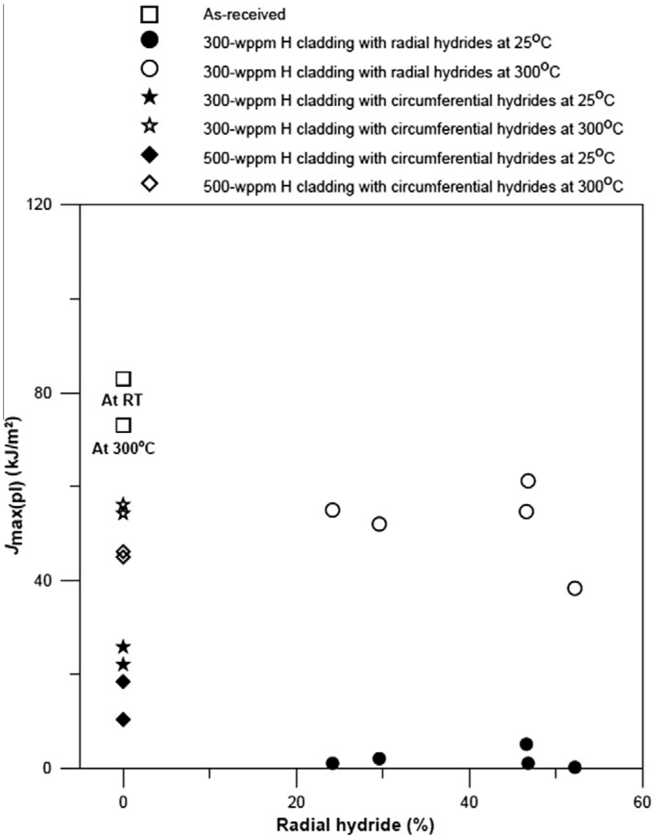

Fig. 8. $J_{max(pl)}$ against the radial hydride percentage for Zry-4 cladding at 25 °C and 300 °C.

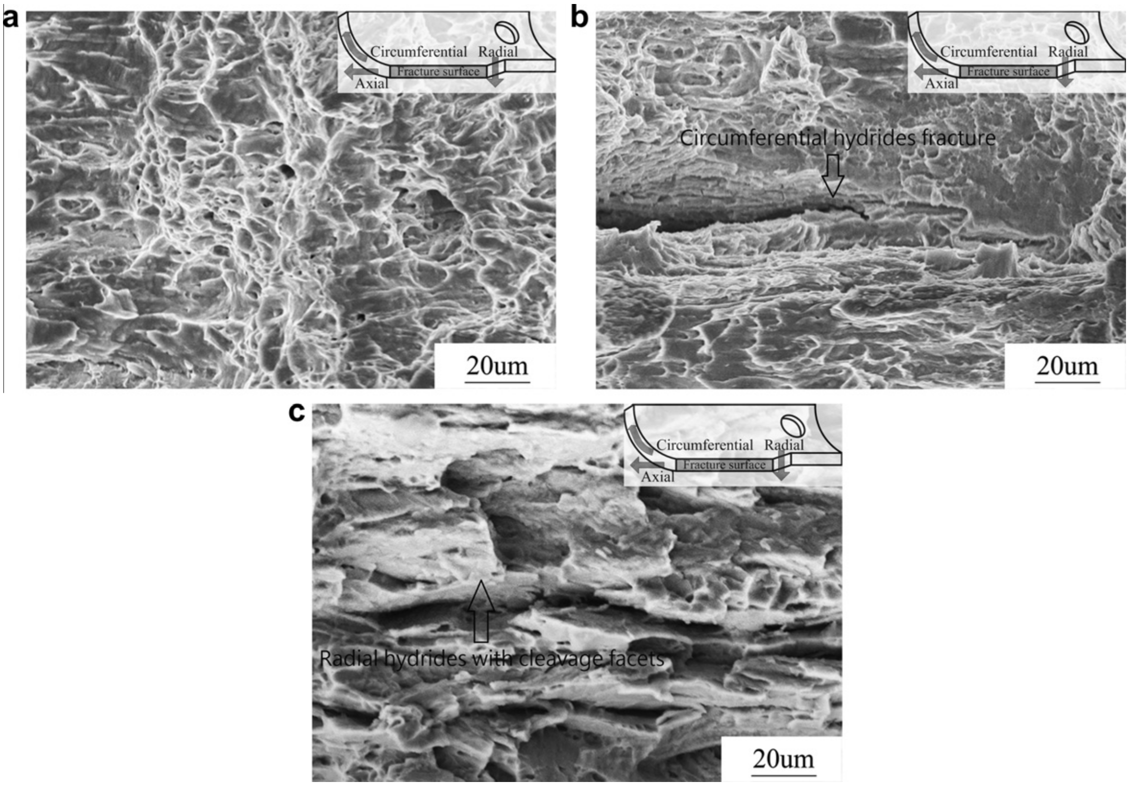

Fig. 9. SEM fractographs of (a) the as-received Zry-4 cladding, (b) 300-wppm hydrogen Zry-4 cladding with circumferential hydrides and (c) 300-wppm hydrogen Zry-4 cladding with 46.6% radial hydrides tested at 25 °C.

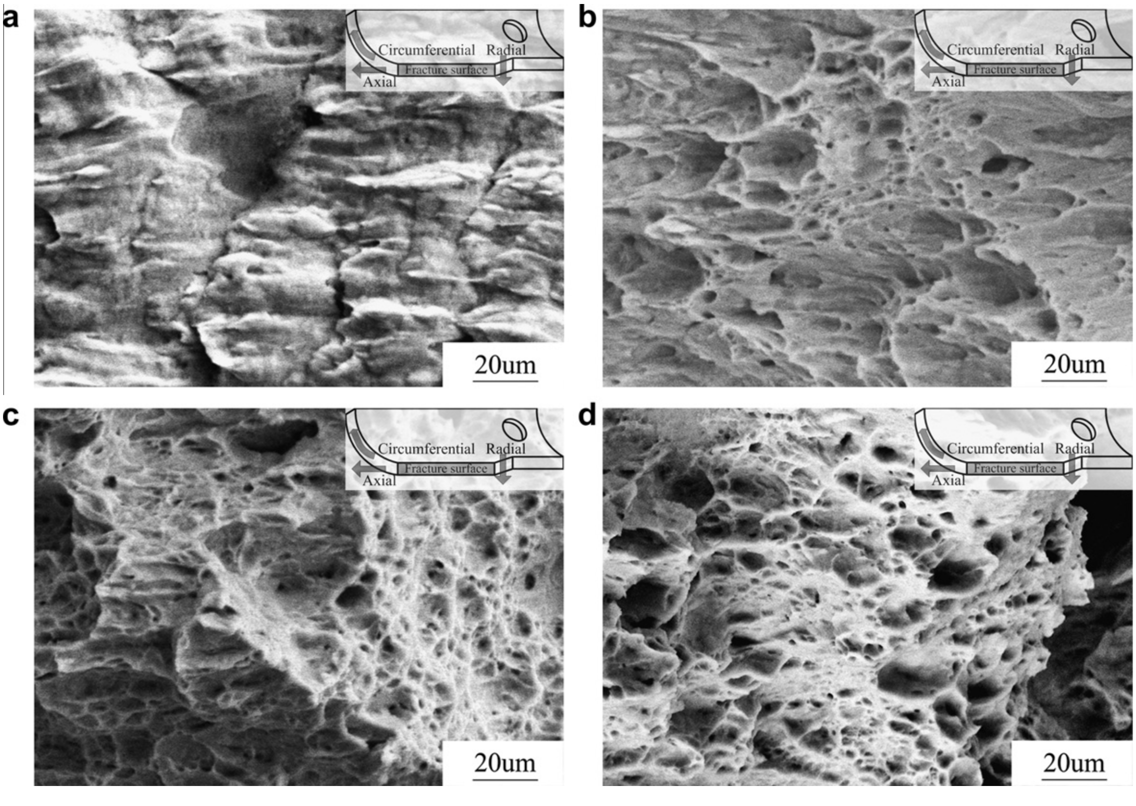

Fig. 10. SEM fractographs of (a) the as-received Zry-4 cladding, (b) 300-wppm hydrogen, (c) 500-wppm hydrogen Zry-4 cladding with circumferential hydrides and (d) 300-wppm hydrogen Zry-4 cladding with 46.6% radial hydrides tested at 300 °C.

toughness relative to the as-received cladding at 300 °C, regardless of whether there existed radial hydrides or not. The $J_{\max}$ values for X-specimens with a hydrogen concentration of 500 wppm at 300 °C were lower than those with circumferential or radial hydrides at 300 wppm hydrogen content. At 300 °C, the fracture toughness for Zry-4 cladding was degraded mainly by the factor of hydrogen concentration, not much by radial hydrides.

3.4. Fractographic analysis

The fracture surfaces of tested samples were further examined using scanning electron microscope (SEM). The fracture surface of the as-received samples tested at 25 °C exhibited typically ductile fracture features of dimples, as shown in Fig. 9a [15]. The observation of the rugged fracture surface accompanying secondary cracks, presented in Fig. 9b, revealed that the specimen with circumferential hydrides failed in a mixed fracture mode. The brittle fracture features of the specimen with radial hydrides indicated that cleavages propagated along the radial hydride platelets, as shown in Fig. 9c. The radial hydride platelets, whose precipitate planes were lying in the radial-axial plane and the plane normal in the direction of applied load, provided a favorable path for crack propagation. The crack would easily proceed along the brittle hydrides or the boundary between the zirconium hydride and metal matrix. Secondary cracks were also visible on the fracture surface but shorter and sparser. At 25 °C, the effect of radial hydride on the degradation of Zry-4 cladding fracture toughness was more significant than circumferential hydride.

The as-received sample tested at 300 °C exhibited fracture features of ductile tearing shown in Fig. 10a. The fracture surfaces of the X-specimens with circumferential hydrides at 300 wppm and 500 wppm, as shown in Figs. 10b and c respectively, indicated that dimples on the fracture surface of the 500-wppm hydrogen X-specimen tested at 300 °C were shallower and more densely populated, relative to those at the 300-wppm hydrogen level. At 300 °C, there were more hydride platelets present in the cladding specimens at higher hydrogen content levels to resist the dislocation motion, and less ductile metallic ligaments to sustain the deformation, both of which could be responsible for lower fracture toughness of heavily hydrided cladding. A comparison of Fig. 10b and d showed that the dimple size on the fracture surfaces was similar for X-specimens in the same hydrogen concentration level with or without radial hydrides. On these accounts, the better ductility of metallic ligaments was inferred to be a dominant factor affecting the fracture toughness of Zry-4 cladding at 300 °C.

4. Conclusions

Hydrogen concentration, hydride orientation and temperature are the factors affecting the fracture toughness of Zr-4 cladding, governing the embrittlement behavior.

1. At 25 °C, the *J*-integral values for 300-wppm hydrogen Zry-4 cladding with radial hydrides are smaller than those with only circumferential hydrides. It can be induced that radial hydrides facilitate crack propagation and degrade the fracture toughness of Zry-4 cladding.
2. At 300 °C, the *J*-integral values for the hydrided Zry-4 cladding at the 300-wppm hydrogen level with radial hydrides are close to those with circumferential hydrides. Although the morphology of the fracture surface is different, the better ductility of zirconium matrix at 300 °C can diminish the extent of embrittlement of Zry-4 cladding induced by zirconium hydrides.

References

[1] C.E. Coleman, D. Hardie, J. Less-Common Met. 11 (1966) 168.
[2] H.H. Hsu, J. Alloys Compd. 426 (2006) 256.
[3] B. Cox, Y.M. Wong, J. Nucl. Mater. 303 (2002) 169.
[4] R.P. Marshall, M.R. Louthan Jr., Trans. ASM 56 (1963) 693.
[5] Y. Mishima, T. Okubo, E. Sano, Metall. Trans. 2 (1971) 1995.
[6] Y. Mishima, T. Okubo, Can. Metall. Q. 11 (1972) 157.
[7] A. Jonsson, L. Hallstadius, B. Grapengiesser, G Lysell, in: Proceedings of the 1991 International Topical Meeting on LWR Fuel Performance, Avignon, France, 21–24 April 1991, p. 371.
[8] H.H. Hsu, K.F. Chien, H.C. Chu, R.C. Kuo, P.K. Liaw, ASTM STP 1406 (2001) 214.
[9] H.C. Chu, S.K. Wu, K.F. Chien, R.C. Kuo, J. Nucl. Mater. 362 (2006) 93.
[10] ASTM, 1997, Standard Test Method for Tension Testing of Metallic Materials, ASTM E1737-96 Annual Book of ASTM Standards, vol. 03.01, ASTM, 1997, p. 968.
[11] A.C. Wallace, G.K. Shek, O.E. Lepik, ASTM STP 1023 (1989) 66.
[12] G.A. Clake, J.D. Landes, J. Test. Eval. 7 (5) (1979) 251.
[13] J.J. Kearns, J. Nucl. Mater. 22 (1967) 292.
[14] P. Vizcaino, A.D. Banchik, J.P. Abriata, J. Nucl. Mater. 304 (2002) 96.
[15] D.O. Northwood, U. Kosasih, Int. Met. Rev. 28 (1983) 92.